Katholieke Universiteit Leuven

Departement Elektrotechniek ESAT-SISTA/TR 2005-243

Adaptive feedback cancellation in hearing aids [1]

Ann Spriet[2], Geert Rombouts[3] ,Marc Moonen[4] ,Jan Wouters[5]

Published the Journal of the Franklin Institute, vol. 343, p. 545–573, 2006

[1] This report is available by anonymous ftp from *ftp.esat.kuleuven.ac.be* in the directory *pub/sista/spriet/reports/05-243.pdf*

[2] K.U.Leuven, Dept. of Electrical Engineering (ESAT), SISTA, Kasteelpark Arenberg 10, 3001 Leuven-Heverlee, Belgium, Tel. 32/16/32 17 95, Fax 32/16/32 19 70. K.U.Leuven, ExpORL, Dept. Neurosciences, O.& N2, Herestraat 49 bus 721, B-3000 Leuven, Belgium. Ann Spriet is a postdoctoral researcher supported by FWO-Vlaanderen. This research work was carried out at the ESAT laboratory and Lab. Exp. ORL of the K. U. Leuven, in the frame of the European project HearCom ('Hearing in the communication society', WP5), the Belgian Programme on Interuniversity Attraction Poles, initiated by the Belgian Federal Science Policy Office IUAP P5/22 ('Dynamical Systems and Control: Computation, Identification and Modelling'), the Concerted Research Action GOA-AMBIORICS ('Algorithms for medical and biological research, integration and software') of the Flemish Government, IWT project 040803 ('SMS4PA-II: Sound Management System for Public Address Systems'). The scientific responsibility is assumed by its authors.

[3] K.U.Leuven, Dept. of Electrical Engineering (ESAT), SISTA, Kasteelpark Arenberg 10, 3001 Leuven-Heverlee, Belgium, Tel. 32/16/32 18 56, Fax 32/16/32 19 70.

[4] K.U.Leuven, Dept. of Electrical Engineering (ESAT), SISTA, Kasteelpark Arenberg 10, 3001 Heverlee, Belgium, Tel. 32/16/32 17 09, Fax 32/16/32 19 70. Marc Moonen is a professor at the Katholieke Universiteit Leuven.

[5] K.U.Leuven, ExpORL, Dept. Neurosciences, O.& N2, Herestraat 49 bus 721, B-3000 Leuven, Belgium, Tel: +32 16 330485, Fax: +32 16 330486. Jan Wouters is a professor at the Katholieke Universiteit Leuven.

Available online at www.sciencedirect.com
ScienceDirect
Journal of the Franklin Institute 343 (2006) 545–573
Journal of The Franklin Institute
www.elsevier.com/locate/jfranklin

Adaptive feedback cancellation in hearing aids

A. Spriet[a,b,*], G. Rombouts[a], M. Moonen[a], J. Wouters[b]

[a]*ESAT/ SCD-SISTA, KU Leuven, Kasteelpark Arenberg 10, B-3001 Leuven, Belgium*
[b]*ExpORL, Department of Neurosciences, KU Leuven, O.&N2, Herestraat 49 bus 721, B-3000 Leuven, Belgium*

Received 28 November 2005; received in revised form 18 July 2006; accepted 22 August 2006

Abstract

In general feedback cancellation setups, standard adaptive filtering techniques fail to provide a reliable feedback path estimate if the desired signal is spectrally colored because of the presence of a closed signal loop. In this paper, several approaches for improving the estimation accuracy of the adaptive feedback canceller in hearing aids will be reviewed, including constrained adaptation and bandlimited adaptation of the feedback canceller as well as adaptation with the prediction-error method (PEM) using a fixed or adaptive model of the desired signal. Partitioned-block frequency-domain implementations of these algorithms will be compared for acoustic feedback paths measured in two commercial behind-the-ear hearing aids. In addition, it is shown that the tracking performance of the PEM-based feedback canceller with adaptive signal model can be improved by the so-called shadow filter approach known from echo cancellation.
© 2006 The Franklin Institute. Published by Elsevier Ltd. All rights reserved.

Keywords: Acoustic feedback; Feedback cancellation; Adaptive; Hearing aids

Contents

1. Introduction 546
2. Standard adaptive feedback canceller 549
   2.1. CAF algorithm and bias 549
   2.2. Partitioned-block frequency-domain (PBFD) LMS implementation 550
3. Adaptive feedback cancellers based on prior knowledge of the acoustic feedback path. . 554
   3.1. Constrained adaptation (C-CAF) 554

*Corresponding author. Tel.: +32 16 321795; fax: +32 16 321970.
E-mail addresses: ann.spriet@esat.kuleuven.be (A. Spriet), geert.rombouts@esat.kuleuven.be (G. Rombouts), marc.moonen@esat.kuleuven.be (M. Moonen), jan.wouters@med.kuleuven.be (J. Wouters).

0016-0032/$30.00 © 2006 The Franklin Institute. Published by Elsevier Ltd. All rights reserved.
doi:10.1016/j.jfranklin.2006.08.002

3.2. Bandlimited adaptation (BL-CAF) . . . 555
4. Adaptive feedback cancellers based on a model of the desired signal (PEMAFC) . . . 558
4.1. Closed-loop identification of the feedback path with the direct method . . . 558
4.2. Desired signal model . . . 559
4.2.1. Fixed desired signal model (PEMAFC-f) . . . 559
4.2.2. Adaptive desired signal model (PEMAFC-a) . . . 561
4.3. Improvement of the tracking performance with the shadow filter approach (PEMAFC-as) . . . 563
5. Simulation results . . . 565
5.1. Performance measures . . . 565
5.2. Simulation results . . . 567
5.2.1. Stationary feedback path . . . 567
5.2.2. Non-stationary feedback path . . . 569
6. Conclusions . . . 570
Acknowledgments . . . 571
References . . . 571

1. Introduction

Acoustic feedback in hearing aids refers to the acoustical coupling between the loudspeaker (also known as the receiver) and the microphone of the hearing aid. Because of this coupling, the hearing aid produces a severe distortion of the desired signal and an annoying howling sound when the gain is increased. With the growing use of open fittings (i.e., without an earmold) to improve listening comfort and the decreasing distance between the loudspeaker and the microphone of the hearing aid (because of the ongoing miniaturization in the hearing aid industry), the demand for effective feedback suppression or cancellation techniques increases.

The problem of acoustic feedback is illustrated in Fig. 1 for a hearing aid with a single microphone. For the notation, we refer to the end of this section. The so-called *forward path* $G(q) = g_0 q^0 + \cdots + g_{L_G-1} q^{-L_G+1}$, where L_G denotes the filter length of $G(q)$, represents the regular signal processing path of the hearing aid (i.e., a frequency-specific gain, compression and/or noise reduction). We assume that $G(q)$ has a delay d_G of at least one sample, i.e., $g_0 = 0$. The *feedback path* between the loudspeaker and the microphone is denoted by $F(q,n)$. The loudspeaker and microphone signals are $u_l[n]$ and $y[n]$, respectively. The desired signal is denoted by $x[n]$ and the feedback signal is denoted by $v[n] = F(q,n)u_l[n]$. Because of acoustic feedback, the amplified sound $u_l[n]$ sent through the

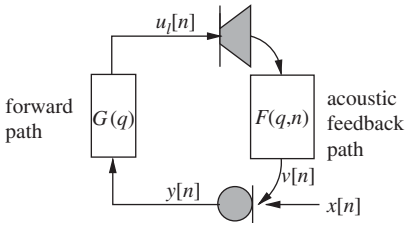

Fig. 1. Acoustic feedback.

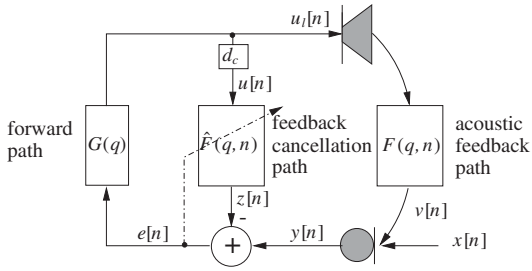

Fig. 2. Adaptive feedback canceller.

loudspeaker is fed back into the microphone, resulting in a closed-loop system

$$\frac{G(q)}{1 - G(q)F(q,n)} \tag{1}$$

from the desired signal $x[n]$ to the loudspeaker signal $u_l[n]$. Instability occurs if the loop gain $|G(e^{j\omega})F(e^{j\omega})|$ exceeds one at an angular frequency $\omega \in [0, \pi]$ where the loop phase equals a multiple of 2π.

To reduce the negative effects introduced by acoustic feedback, several techniques have been proposed in the literature. They can be broadly classified into feedforward suppression and feedback cancellation techniques. In *feedforward suppression* techniques, the regular signal processing path $G(q)$ of the hearing aid is modified in such a way that it is stable in conjunction with the feedback path $F(q,n)$. The most common technique is the use of a notch filter. In a notch filter, the gain is reduced in a narrow frequency band around the critical frequencies, whenever feedback occurs [1–4]. Other examples include equalizing the phase of the open-loop response [5] and using time-varying elements such as frequency shifting, delay and phase modulation, in the forward path [1,6,7]. The achievable increase in maximum stable gain with feedforward suppression techniques has generally been found to be limited [1,6]. In addition, feedforward suppression techniques all compromise the basic frequency response of the hearing aid, and, hence, may seriously affect the sound quality.

A more promising solution for acoustic feedback is the use of a *feedback cancellation* algorithm, which is described in Fig. 2. The feedback canceller $\hat{F}(q,n)$ produces an estimate $z[n]$ of the feedback signal $v[n]$ and subtracts this estimate $z[n]$ from the microphone signal, so that, ideally, only the desired signal is preserved at the input of $G(q)$.[1] Since the acoustic path between the loudspeaker and the microphone can vary significantly depending on the acoustical environment [8–11], the feedback canceller must be adaptive. Currently available adaptive feedback cancellers can be divided into two classes: algorithms with a continuous adaptation and algorithms with a *non-continuous adaptation* [3,12,13]. The latter adapt the coefficients of the feedback canceller only when instability is detected or when the input signal level is low [13–15]. Due to this reactive, rather than proactive, adaptation, such systems may be objectionable. A *continuous adaptation* feedback (CAF) canceller continuously adapts the coefficients of the feedback path estimate in such a way that the energy of the feedback-compensated signal is minimized. This is depicted in Fig. 2.

[1]The integer delay d_c in Fig. 2 models the delay in the acoustic feedback path $F(q,n)$ (cf. Section 2.1).

However, the adaptive modelling problem encountered here appears to be highly non-trivial, because of the presence of a closed signal loop (i.e., the forward path) that introduces a specific signal correlation (cf. Section 2.1). As a result, the standard CAF cancellers fail to provide a reliable ('unbiased') feedback path estimate, when the desired signal $x[n]$ is spectrally colored.

In this paper, several approaches for improving the estimation accuracy of the adaptive feedback canceller will be reviewed and compared. We concentrate on techniques that do not require the use of an external noise signal during adaptation. A first class of techniques controls the adaptation of the feedback canceller, i.e., applies constrained adaptation or bandlimited adaptation. These techniques are based on prior knowledge of the acoustic feedback path. A second class of techniques reduces the bias of the feedback path estimate by exploiting a fixed or adaptive model of the desired signal. The feedback canceller is then adapted using the prediction-error method (PEM). To improve convergence, these algorithms are transformed to the frequency domain. Partitioned-block techniques will be used to limit the total processing delay, which in a hearing aid should not exceed 10–20 ms in order not to degrade intelligibility [16] and sound quality [17,18]. The algorithms will be compared for acoustic feedback paths measured in two commercial behind-the-ear (BTE) hearing aids. In addition, it will be shown that the tracking performance of the PEM-based adaptive feedback canceller (PEMAFC) can be improved by the so-called shadow filter approach known from echo cancellation [19].

The paper is organized as follows. Section 2 reviews the problem of standard adaptive feedback cancellation techniques. We show that the standard feedback cancellation algorithm suffers from a model error or bias when the desired signal is spectrally colored. Sections 3 and 4 discuss solutions to improve the estimation accuracy of the standard adaptive feedback canceller. In Section 3, feedback cancellation with constrained adaptation and bandlimited adaptation is described. Section 4 discusses feedback cancellation based on the PEM and modelling of the desired signal. In addition, it is shown that the tracking performance of the PEMAFC can be improved by putting a second faster adaptive filter (so-called shadow filter) in parallel to the feedback canceller. Partitioned-block frequency-domain (PBFD) LMS implementations of the algorithms are compared in Section 5 for feedback paths measured in two commercial BTEs mounted on an artificial head. The simulations show that incorporating prior knowledge of the feedback path (through constrained or bandlimited adaptation) as well as exploiting an estimate of the desired signal in the adaptation improve the estimation accuracy of the standard feedback canceller. Thanks to a pre-whitening of the desired signal, the feedback cancellers based on a model of the desired signal exhibit a faster convergence than the feedback cancellers with constrained or bandlimited adaptation. In addition, we show that the shadow filter approach further improves the tracking performance of the PEMAFC with adaptive signal model. The PEMAFC with shadow filter combines a slow and a fast adaptive filter, resulting in a faster tracking of feedback path changes, while preserving a good steady-state performance.

Notation: Throughout this paper, the following notation is used.

The superscripts T and H denote matrix/vector transpose and complex conjugate transpose, respectively. The expectation operator is denoted by $\varepsilon\{\cdot\}$. The matrix $\mathscr{F}$ is the $M \times M$ DFT matrix. The matrix $\mathbf{I}_L$ is the $L \times L$ identity matrix. The matrix $\mathbf{0}_L$ is an $L \times L$ dimensional matrix of zeros.

The discrete-time index is denoted by n. The symbol q^{-1} denotes the discrete-time delay operator, i.e.,

$$q^{-1}u[n] = u[n-1]. \tag{2}$$

A discrete-time filter with coefficient vector $\mathbf{f}[n]$,

$$\mathbf{f}[n] = [f_0[n]\ f_1[n]\ \cdots\ f_{L_F-1}[n]]^{\mathrm{T}}, \tag{3}$$

and filter length L_F is represented as a polynomial transfer function $F(q,n)$ in q, i.e.,

$$F(q,n) = \mathbf{f}^{\mathrm{T}}[n]\mathbf{q}, \tag{4}$$

with $\mathbf{q} = [1\ \ q^{-1}\ \ \ldots\ \ q^{-L_F+1}]^{\mathrm{T}}$. This representation, which is adopted from [20], allows the following notation for the filtering of $u[n]$ with $F(q,n)$:

$$F(q,n)u[n] = \mathbf{f}^{\mathrm{T}}[n]\mathbf{u}[n], \tag{5}$$

with

$$\mathbf{u}[n] = [u[n]\ \ u[n-1]\ \ \cdots\ \ u[n-L_F+1]]^{\mathrm{T}}. \tag{6}$$

The spectrum of $F(q,n)$ is denoted by $F(\mathrm{e}^{\mathrm{j}\omega})$ with $\omega \in [0,\pi]$ the normalized angular frequency.

2. Standard adaptive feedback canceller

2.1. CAF algorithm and bias

The standard CAF $\hat{\mathbf{f}}[n] = [f_0[n]\ f_1[n]\ \cdots\ f_{L_{\hat{F}}}[n]]^{\mathrm{T}}$ continuously adapts the coefficients of the feedback canceller based on standard adaptive filtering (Wiener filtering) procedures. The standard CAF minimizes

$$J(\hat{\mathbf{f}}[n]) = \varepsilon\{|y[n] - \hat{\mathbf{f}}^{\mathrm{T}}[n]\mathbf{u}[n]|^2\}, \tag{7}$$

with $\mathbf{u}[n] = [u[n]\ \ u[k-1]\ \ \cdots\ \ u[k-L_{\hat{F}}+1]]^{\mathrm{T}}$ and $u[n] = u_{\mathrm{l}}[n-d_{\mathrm{c}}]$ (cf. Fig. 2), resulting in the well-known Wiener filter

$$\hat{\mathbf{f}}[n] = \varepsilon\{\mathbf{u}[n]\mathbf{u}^{\mathrm{T}}[n]\}^{-1}\varepsilon\{\mathbf{u}[n]y[n]\}. \tag{8}$$

Typically the acoustic feedback path $F(q,n)$ contains a delay d_{c} that arises from the processing delay of the ADC and DAC converters, i.e., $F(q,n) = q^{-d_{\mathrm{c}}}\tilde{F}(q,n)$ with $L_F = d_{\mathrm{c}} + L_{\tilde{F}}$ such that $F(q,n)u_{\mathrm{l}}[n] = \tilde{\mathbf{f}}[n]^{\mathrm{T}}\mathbf{u}[n]$. To reduce complexity, the feedback path $F(q,n)$ is therefore modelled as a cascade of a delay d_{c} and a shorter feedback canceller $\hat{F}(q,n)$.

In the sequel, we focus on the sufficient-order case, where $L_{\hat{F}} = L_F - d_{\mathrm{c}}$. Then, using

$$y[n] = \tilde{\mathbf{f}}^{\mathrm{T}}[n]\mathbf{u}[n] + x[n], \tag{9}$$

the feedback path estimate $\hat{\mathbf{f}}[n]$ can be decomposed as

$$\begin{aligned}\hat{\mathbf{f}}[n] &= \varepsilon\{\mathbf{u}[n]\mathbf{u}^{T}[n]\}^{-1}(\varepsilon\{\mathbf{u}[n]\mathbf{u}^{\mathrm{T}}[n]\tilde{\mathbf{f}}[n]\} + \varepsilon\{\mathbf{u}[n]x[n]\}) \\ &= \tilde{\mathbf{f}}[n] + \varepsilon\{\mathbf{u}[n]\mathbf{u}^{\mathrm{T}}[n]\}^{-1}\varepsilon\{\mathbf{u}[n]x[n]\}.\end{aligned} \tag{10}$$

If $\varepsilon\{\mathbf{u}[n]x[n]\} = \mathbf{0}$, the feedback path estimate is unbiased.

However, because of the presence of the closed signal loop $G(q)$, the input signal $u[n]$ to the adaptive filter $\hat{\mathbf{f}}[n]$ relates to $x[n]$ as

$$u[n] = q^{-d_c} C(q,n)x[n] = \frac{q^{-d_c} G(q)}{1 - G(q)(F(q,n) - q^{-d_c}\hat{F}(q,n))} x[n], \tag{11}$$

where $C(q,n)$ is the transfer function from $x[n]$ to the loudspeaker signal $u_l[n]$. Assume that $G(q)$ contains a delay $d_G \in \mathbb{N}$ with $d_G \geqslant 1$ and assume that $G(q)$, $F(q,n)$ and $\hat{F}(q,n)$ are causal. Then, the closed-loop system $C(q,n)$ can be specified as

$$C(q,n) = c_{d_G}[n]q^{-d_G} + c_{d_G+1}[n]q^{-d_G-1} + \cdots + c_{L_C-1}[n]q^{-L_C+1} \tag{12}$$

and hence

$$u[n] = (c_{d_G}[n] + \cdots + c_{L_C-1}[n]q^{-L_C+d_G+1})x[n - d_G - d_c]. \tag{13}$$

As a result, $\varepsilon\{\mathbf{u}[n]x[n]\} = \mathbf{0}$ if and only if

$$\varepsilon\{x[n-\delta]x[n]\} = 0 \tag{14}$$

for $d_G + d_c \leqslant \delta \leqslant L_C + L_{\hat{F}} + d_c - 2$.

Most practical sound signals $x[n]$ are *spectrally colored*, meaning that the signal values $x[n]$ are correlated in time (e.g., speech, music, etc). Many of these audio signals may be well approximated as low-order, autoregressive (AR) random processes,

$$x[n] = H(q)w[n] = \frac{1}{1 + q^{-1}\bar{A}(q)} w[n], \tag{15}$$

with $w[n]$ a white noise signal. Hence, the signal model $H(q)$ is often IIR, so that the length L_H of $H(q)$ exceeds $d_G + d_c$ and hence, $\varepsilon\{\mathbf{u}[n]x[n]\} \neq 0$. The CAF will then cancel the desired signal $x[n]$ instead of the feedback signal $v[n] = \tilde{F}(q,n)u[n]$ (see Eq. (10)), leading to signal distortion. From Eq. (10), we observe that the bias in the feedback path estimate decreases with an increasing power ratio of the feedback signal $v[n]$ (i.e., the signal to identify) to the desired signal $x[n]$ (which acts as a disturbance). Since $v[n] = F(q,n)C(q,n)x[n]$ with $C(q,n)$ defined in Eq. (11), the larger the loop gain $|G(q)F(q,n)|$, the smaller the bias will be. This indicates that the bias will be smallest for large gains $G(q)$ and for frequencies that are closest to instability. In Sections 3 and 4, solutions for reducing the bias of the CAF will be discussed.

2.2. Partitioned-block frequency-domain (PBFD) LMS implementation

Standard adaptive filtering procedures (e.g., LMS, RLS) can be used for adapting the filter coefficients $\hat{\mathbf{f}}[n]$ of the CAF. In this paper, we use a PBFD LMS implementation based on an overlap-save procedure [21–23]. PBFD adaptive filters combine the beneficial properties of frequency-domain algorithms, i.e., a frequency-dependent step size control, faster convergence (thanks to the decorrelation properties of the FFT) and a reduced complexity, with a small processing delay as required for hearing aid applications.

In the overlap-save PBFD LMS adaptive algorithm, the $L_{\hat{F}}$-taps feedback canceller $\hat{\mathbf{f}}[n]$ is partitioned into $L_{\hat{F}}/P$ segments $\hat{\mathbf{f}}_p[n]$ of length P each, which are then transformed to the

frequency domain[2]:

$$\hat{\mathbf{f}}_p[n] = [\hat{f}_{pP}[n]\ \hat{f}_{pP+1}[n]\ \cdots\ \hat{f}_{(p+1)P-1}[n]]^{\mathrm{T}}, \tag{16}$$

$$\hat{\mathbf{F}}_p[n] = \mathscr{F}\begin{bmatrix}\hat{\mathbf{f}}_p[n]\\ \mathbf{0}\end{bmatrix}\begin{matrix}\updownarrow P\\ \updownarrow M-P\end{matrix} \quad \forall p = 0 : \frac{L_{\hat{F}}}{P} - 1, \tag{17}$$

where $\mathscr{F}$ equals the $M \times M$ DFT matrix.

Define the L-dimensional block signal $\mathbf{u}_m$ as

$$\mathbf{u}_m = [u[mL+1]\ \ldots\ u[(m+1)L]]^{\mathrm{T}}, \tag{18}$$

where m is the block time index. For each block $\mathbf{u}_m$ of input samples, the PBFD LMS filter produces L output samples $\mathbf{z}_m = [z[mL+1]\ \ldots\ z[(m+1)L]]^{\mathrm{T}}$:

$$\mathbf{U}_p[m] = \mathrm{diag}\left\{\mathscr{F}\begin{bmatrix}u[(m+1)L - pP - M + 1]\\ \vdots\\ u[(m+1)L - pP]\end{bmatrix}\right\} \quad \forall p = 0 : \frac{L_{\hat{F}}}{P} - 1, \tag{19}$$

$$\mathbf{z}_m = \begin{bmatrix}\mathbf{0} & \mathbf{I}_L\end{bmatrix}\mathscr{F}^{-1}\sum_{p=0}^{L_{\hat{F}}/P-1}\mathbf{U}_p[m]\hat{\mathbf{F}}_p[m]. \tag{20}$$

Parameter L is called the blocklength and, hence, the corresponding input/output delay of the PBFD implementation equals $2L-1$. To ensure proper operation, it is required that the DFT length $M \geqslant P + L - 1$. The LMS adaptive filter coefficients are updated based on overlap-save:

$$\mathbf{E}[m] = \mathscr{F}\begin{bmatrix}\mathbf{0}\\ \mathbf{e}_m\end{bmatrix}\begin{matrix}\updownarrow M-L\\ \updownarrow L\end{matrix}, \quad \mathbf{e}_m = \mathbf{y}_m - \mathbf{z}_m, \tag{21}$$

$$\mathbf{y}_m = [y[mL+1]\ \ldots\ y[(m+1)L]]^{\mathrm{T}}, \tag{22}$$

$$\hat{\mathbf{F}}_p[m+1] = \hat{\mathbf{F}}_p[m] + \boldsymbol{\Delta}[m]\mathscr{F}\mathbf{g}\mathscr{F}^{-1}\mathbf{U}_p^{\mathrm{H}}[m]\mathbf{E}[m], \tag{23}$$

where

$$\mathbf{g} = \begin{bmatrix}\mathbf{I}_P & \mathbf{0}\\ \mathbf{0} & \mathbf{0}_{M-P}\end{bmatrix} \tag{24}$$

and where $\boldsymbol{\Delta}[m]$ is a diagonal matrix that contains the step sizes $\mu_k[m]$, $k = 0, \ldots, M-1$ of the different frequency bins k, i.e.,

$$\boldsymbol{\Delta}[m] = \mathrm{diag}\{\mu_0[m], \ldots, \mu_{M-1}[m]\}. \tag{25}$$

Each step size $\mu_k[m]$ is normalized according to the sum of the input power $P_{u,k}[m]$ and the error power $P_{e,k}[m]$ in each frequency bin k [21,24]:

$$\mu_k[m] = \frac{\bar{\mu}_k}{P_{u,k}[m] + P_{\mathrm{e},k}[m]}, \quad k = 0, \ldots, M-1, \tag{26}$$

[2]It is assumed that $L_{\hat{F}}/P \in \mathbb{N}_0$. Otherwise $\hat{\mathbf{f}}_p[n]$ has to be padded with zeros.

with

$$P_{u,k}[m] = \sum_{p=0}^{L_{\hat{F}}/P-1} |U_{p,k}[m]|^2,$$

$$P_{\mathrm{e},k}[m] = \frac{L_{\hat{F}}}{P} |E_{p,k}[m]|^2. \tag{27}$$

This normalization of the step size with the sum of the input and error power reduces the excess error in the presence of desired signals with large power fluctuations and signal onsets. For a highly time-varying desired signal $x[n]$ such as a speech signal, a burst in the error signal $e[n]$ mostly originates from fluctuations in the short-time power of $x[n]$. Normalization with the input and error power reduces the step size $\mu_k[m]$, when the desired signal $x[n]$ is strong and, hence, mitigates the negative effect of a strong desired signal segment on the excess mean squared error. To avoid excessive step sizes in poorly excited frequency bins, the input and error power are constrained according to the average power in a band of neighboring bins [21]. The frequency bins are grouped in K subbands $\{B_i\}_{i\in[1;K]}$. In each band B_i, the mean input and error power $P_{u,B_i}[m]$ and $P_{\mathrm{e},B_i}[m]$ are computed as:

$$P_{u,B_i}[m] = \mathrm{mean}\{P_{u,k}[m]\}_{(k\in B_i)} \quad P_{\mathrm{e},B_i}[m] = \mathrm{mean}\{P_{\mathrm{e},k}[m]\}_{(k\in B_i)}. \tag{28}$$

The $P_{u,B_i}[m]$ and $P_{\mathrm{e},B_i}[m]$ are then used as a maximum threshold for $P_{u,k}[m]$ and $P_{\mathrm{e},k}[m]$ with $k \in B_i$:

$$\mu_k[m] = \frac{\bar{\mu}_k}{\max(P_{u,k}[m], P_{u,B_i}[m]) + \max(P_{\mathrm{e},k}[m], P_{\mathrm{e},B_i}[m])}. \tag{29}$$

The PBFD implementation of the CAF is summarized in Algorithm 1 and illustrated in Fig. 3.

Algorithm 1. PBFD implementation of CAF.

For each block of L input samples $u[mL+1],\ldots,u[(m+1)L]$:

$$\mathbf{U}_p[m] = \mathrm{diag}\left\{ \mathscr{F} \begin{bmatrix} u[(m+1)L - pP - M + 1] \\ \vdots \\ u[(m+1)L - pP] \end{bmatrix} \right\} \quad \forall p = 0 : \frac{L_{\hat{F}}}{P} - 1.$$

Block of output samples $\mathbf{z}_m = [z[mL+1]\ldots z[(m+1)L]]^{\mathrm{T}}$:

$$\mathbf{z}_m = [\,\mathbf{0} \quad \mathbf{I}_L\,]\mathscr{F}^{-1} \sum_{p=0}^{L_{\hat{F}}/P-1} \mathbf{U}_p[m]\hat{\mathbf{F}}_p[m].$$

Update formula:

$$\mathbf{y}_m = [y[mL+1] \ \ldots \ y[(m+1)L]]^{\mathrm{T}},$$

$$\mathbf{E}[m] = \mathscr{F} \begin{bmatrix} \mathbf{0} \\ \mathbf{I}_L \end{bmatrix} \left(\mathbf{y}_m - \begin{bmatrix} \mathbf{0} & \mathbf{I}_L \end{bmatrix} \mathscr{F}^{-1} \sum_{p=0}^{L_{\hat{F}}/P-1} \mathbf{U}_p[m]\hat{\mathbf{F}}_p[m] \right),$$

$$\hat{\mathbf{F}}_p[m+1] = \hat{\mathbf{F}}_p[m] + \mathbf{\Delta}[m]\mathscr{F}\mathbf{g}\mathscr{F}^{-1}\mathbf{U}_p^{\mathrm{H}}[m]\mathbf{E}[m].$$

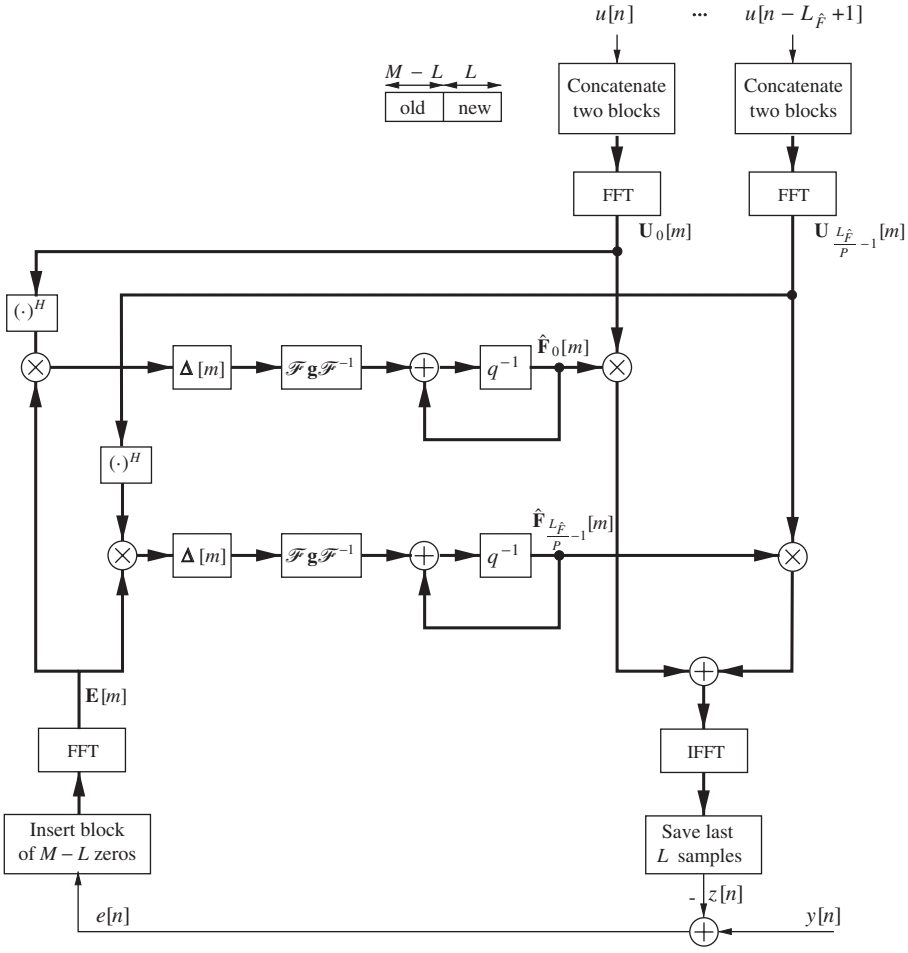

Fig. 3. Block diagram of the PBFD implementation of CAF.

The distortion of the desired signal by the CAF can be reduced by using a slower adaptation speed $\bar{\mu}_k$ in frequency regions where the feedback signal to desired signal power ratio is low (cf. Section 2.1) or equivalently, in frequency bins with a small loop gain $|G(q)F(q,n)|$. A slow adaptation speed reduces the ability to track changes in the spectrum of the desired signal $x[n]$, and, hence, limits the negative effect of a signal with a temporarily strong autocorrelation on the feedback path estimate [18,25–27]. However, this goes at the expense of a reduced convergence and hence, a degraded ability to model feedback path variations in these frequency bins. In this paper, the step sizes $\bar{\mu}_k$ are set to

$$\begin{aligned}\bar{\mu}_0 &= 0.0002,\\ \bar{\mu}_k &= 0.002 \quad \text{for } k = 1,\ldots,3,\\ &= 0.008 \quad \text{for } k = 4,\ldots,\left\lfloor \frac{M}{2}+1 \right\rfloor,\end{aligned} \tag{30}$$

where $\lfloor x \rfloor$ denotes the largest integer smaller than or equal to x.

3. Adaptive feedback cancellers based on prior knowledge of the acoustic feedback path

In [28–30], prior knowledge of the acoustic feedback path is exploited to reduce the bias of the standard CAF. The adaptation of the feedback canceller is controlled based on the prior knowledge through constrained or bandlimited adaptation.

3.1. Constrained adaptation (C-CAF)

In [29,30], the bias is reduced by constrained adaptation: the filter coefficients $\hat{\mathbf{f}}[n]$ of the adaptive feedback canceller $\hat{F}(q,n)$ are not allowed to deviate too far from reference filter coefficients $\hat{\mathbf{f}}_{\text{ref}}$, which are measured during start-up or fitting by means of a probe signal (noise signal).

A cheap method to impose this constraint is to add a term to the cost function (7) of the feedback canceller that penalizes excessive deviation of the filter $\hat{\mathbf{f}}[n]$ from the reference filter $\hat{\mathbf{f}}_{\text{ref}}$, i.e.,

$$J(\hat{\mathbf{f}}[n]) = \varepsilon\{|y[n] - \hat{\mathbf{f}}^{\mathrm{T}}[n]\mathbf{u}[n]|^2\} + \eta(\hat{\mathbf{f}}[n] - \hat{\mathbf{f}}_{\text{ref}})^{\mathrm{T}}(\hat{\mathbf{f}}[n] - \hat{\mathbf{f}}_{\text{ref}}), \tag{31}$$

where the scalar η trades off between signal distortion reduction and the ability to model deviations from $\hat{\mathbf{f}}_{\text{ref}}$. This results in a time-domain, NLMS update equation:

$$\hat{\mathbf{f}}[n+1] = \hat{\mathbf{f}}[n] + \frac{\bar{\mu}}{p_u + p_e + \eta}[\mathbf{u}[n](y[n] - \hat{\mathbf{f}}^{\mathrm{T}}[n]\mathbf{u}[n]) - \eta(\hat{\mathbf{f}}[n] - \hat{\mathbf{f}}_{\text{ref}})]. \tag{32}$$

Converting Eq. (32) into the frequency domain, results in the following PBFD update equation:

$$\hat{\mathbf{F}}_p[m+1] = \hat{\mathbf{F}}_p[m] + \boldsymbol{\Delta}[m](\mathscr{F}\mathbf{g}\mathscr{F}^{-1}\mathbf{U}_p^{\mathrm{H}}[m]\mathbf{E}[m] - \boldsymbol{\eta}(\hat{\mathbf{F}}_p[m] - \hat{\mathbf{F}}_{p,\text{ref}})), \tag{33}$$

where

$$\hat{\mathbf{f}}_{p,\text{ref}} = [\hat{f}_{\text{ref},pP}\ \hat{f}_{\text{ref},pP+1}\ \cdots\ \hat{f}_{\text{ref},(p+1)P-1}]^{\mathrm{T}}, \tag{34}$$

$$\hat{\mathbf{F}}_{p,\text{ref}} = \mathscr{F}\begin{bmatrix} \hat{\mathbf{f}}_{p,\text{ref}} \\ \mathbf{0} \end{bmatrix} \begin{matrix} \updownarrow P \\ \updownarrow M-P \end{matrix} \quad \forall p = 0 : \frac{L_{\hat{F}_{\text{ref}}}}{P} - 1, \tag{35}$$

$$\boldsymbol{\Delta}[m] = \text{diag}\{\mu_0[m], \ldots, \mu_{M-1}[m]\} \tag{36}$$

with

$$\mu_k[m] = \frac{\bar{\mu}_k}{P_{u,k}[m] + P_{e,k}[m] + \eta_k}, \quad k = 0, \ldots, M-1, \tag{37}$$

and where $\boldsymbol{\eta}$ is now a diagonal matrix that contains the trade-off parameters η_k, $k = 0, \ldots, M-1$, of the different frequency bins k. In this paper, η_k, $k = 0, \ldots, M-1$, are set to 0.05. The reference filter coefficients $\hat{\mathbf{f}}_{p,\text{ref}}$ are computed by disconnecting the forward path $G(q)$ and inserting a white noise signal into the loudspeaker. The filter length $L_{\hat{F}_{\text{ref}}}$ of the reference filter is 20. Algorithm 2 summarizes the C-CAF.

Algorithm 2. PBFD implementation of C-CAF.

For each block of L input samples $u[mL+1],\ldots,u[(m+1)L]$:

$$\mathbf{U}_p[m]=\operatorname{diag}\left\{\mathscr{F}\begin{bmatrix}u[(m+1)L-pP-M+1]\\ \vdots\\ u[(m+1)L-pP]\end{bmatrix}\right\}\quad \forall p=0:\frac{L_{\hat{F}}}{P}-1.$$

Block of output samples $\mathbf{z}_m=[z[mL+1]\ldots z[(m+1)L]]^{\mathrm{T}}$:

$$\mathbf{z}_m=\begin{bmatrix}\mathbf{0} & \mathbf{I}_L\end{bmatrix}\mathscr{F}^{-1}\sum_{p=0}^{L_{\hat{F}}/P-1}\mathbf{U}_p[m]\hat{\mathbf{F}}_p[m].$$

Update formula:

$$\mathbf{y}_m=[y[mL+1]\ \ \ldots\ \ y[(m+1)L]]^{\mathrm{T}},$$

$$\mathbf{E}[m]=\mathscr{F}\begin{bmatrix}\mathbf{0}\\ \mathbf{I}_L\end{bmatrix}\left(\mathbf{y}_m-[\mathbf{0}\ \ \mathbf{I}_L]\mathscr{F}^{-1}\sum_{p=0}^{L_{\hat{F}}/P-1}\mathbf{U}_p[m]\hat{\mathbf{F}}_p[m]\right),$$

$$\hat{\mathbf{F}}_p[m+1]=\hat{\mathbf{F}}_p[m]+\boldsymbol{\Delta}[m](\mathscr{F}\mathbf{g}\mathscr{F}^{-1}\mathbf{U}_p^{\mathrm{H}}[m]\mathbf{E}[m]-\boldsymbol{\eta}(\hat{\mathbf{F}}_p[m]-\hat{\mathbf{F}}_{p,\mathrm{ref}})).$$

3.2. Bandlimited adaptation (BL-CAF)

To avoid instability, it suffices that the feedback canceller cancels the feedback signal at or near the critical frequencies, where instability is about to occur. In [27,28,31], feedback cancellation is therefore restricted to the frequency band that encompasses the unstable frequencies. Typically, the feedback path of a hearing aid provides less attenuation at high frequencies [32], where most hearing aid users have the largest hearing loss. As a result, the risk for unstable acoustic feedback is often highest in the high-frequency range, while most of the desired signal energy is typically concentrated at low frequencies, e.g., for speech signals. By concentrating the adaptation of the feedback canceller on the higher frequencies only, the feedback canceller may be more efficient and will introduce less distortion.

Fig. 4 depicts the block diagram of a bandlimited feedback canceller. The filters $B_1(q)$ and $B_2(q)$ are high-pass or band pass filters chosen such that all critical frequencies are preserved while other desired signal components are removed as much as possible. The filter $B_1(q)$ in the feedback cancellation path limits the feedback cancellation signal to the frequency band of interest and, hence, prevents the desired signal components outside the critical band from being distorted by the feedback canceller $\hat{F}(q,n)$. To focus the modelling effort of the adaptive feedback canceller $\hat{\mathbf{f}}[n]$ on the regions that contain the critical frequencies, the adaptive filter $\hat{\mathbf{f}}[n]$ minimizes the frequency-weighted error energy,

$$\begin{aligned}J(\hat{\mathbf{f}}[n])&=\varepsilon\{|B_2(q)(y[n]-\hat{F}(q,n)u^{BP_1}[n])|^2\}\\&=\varepsilon\{|y^{\mathrm{f}}[n]-\hat{F}(q,n)u^{\mathrm{f}}[n]|^2\},\end{aligned}\tag{38}$$

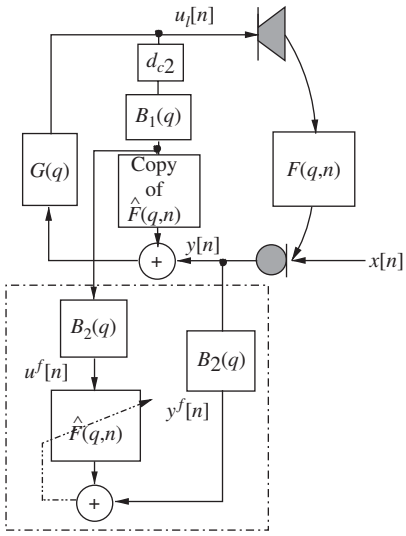

Fig. 4. Bandlimited adaptive feedback cancellation.

where $u^{BP_1}[n] = B_1(q)u[n]$, $y^f[n] = B_2(q)y[n]$ and $u^f[n] = B_2(q)u^{BP_1}[n]$. In [28], the optimization criterion (38) is realized through a filtered-X algorithm. In the filtered-X algorithm, the input signal $u^{BP_1}[n]$ and the feedback-compensated signal $y[n] - \hat{F}(q)u^{BP_1}[n]$ are filtered by $B_2(q)$ before being used to adapt the adaptive filter $\hat{F}(q,n)$. From Eq. (38), it follows that $J(\hat{\mathbf{f}}[n])$ can equivalently be optimized by performing standard adaptive filtering techniques on the pre-filtered microphone and loudspeaker data $y^f[n]$ and $u^f[n]$. In contrast to the filtered-X algorithm, any change to the adaptive filter $\hat{\mathbf{f}}[n]$ then has an immediate effect on the frequency-weighted error so that no stability problems may occur when $B_2(q)$ has a large group delay [28,33]. When using the PBFD procedure, the update equation corresponds to

$$\mathbf{U}_p^f[m] = \mathrm{diag}\left\{ \mathscr{F} \begin{bmatrix} u^f[(m+1)L - pP - M + 1] \\ \vdots \\ u^f[(m+1)L - pP] \end{bmatrix} \right\} \quad \forall p = 0 : \frac{L_{\hat{F}}}{P} - 1, \tag{39}$$

$$\mathbf{y}_m^f = [y^f[mL+1] \ \ \ldots \ \ y^f[(m+1)L]]^T, \tag{40}$$

$$\mathbf{E}^f[m] = \mathscr{F} \begin{bmatrix} \mathbf{0} \\ \mathbf{I}_L \end{bmatrix} \left(\mathbf{y}_m^f - [\mathbf{0} \ \ \mathbf{I}_L]\mathscr{F}^{-1} \sum_{p=0}^{L_{\hat{F}}/P-1} \mathbf{U}_p^f[m]\hat{\mathbf{F}}_p[m] \right), \tag{41}$$

$$\hat{\mathbf{F}}_p[m+1] = \hat{\mathbf{F}}_p[m] + \mathbf{\Delta}[m]\mathscr{F}\mathbf{g}\mathscr{F}^{-1}\mathbf{U}_p^{f,H}[m]\mathbf{E}^f[m] \tag{42}$$

with

$$\mathbf{\Delta}[m] = \mathrm{diag}\{\mu_0[m], \ldots, \mu_{M-1}[m]\}. \tag{43}$$

Again, the step sizes are normalized according to the input and error power in each frequency bin:

$$\mu_k[m] = \frac{\bar{\mu}_k}{P_{u^{\mathrm{f}},k}[m] + P_{e^{\mathrm{f}},k}[m]}, \quad k = 0, \ldots, M-1, \tag{44}$$

$$P_{u^{\mathrm{f}},k}[m] = \sum_{p=0}^{L_{\hat{F}}/P-1} |U_{p,k}^{\mathrm{f}}[m]|^2, \tag{45}$$

$$P_{e^{\mathrm{f}},k}[m] = \frac{L_{\hat{F}}}{P} |E_{p,k}^{\mathrm{f}}[m]|^2. \tag{46}$$

Since the energy of the residual error signal (which acts as a disturbance to the adaptive feedback canceller) is reduced by the high-pass filter $B_2(q)$, the misadjustment of the bandlimited adaptive feedback canceller is reduced compared to the standard CAF. The PBFD implementation of the BL-CAF is summarized in Algorithm 3.

Algorithm 3. PBFD implementation of BL-CAF.

For each block of L input samples $u[mL+1], \ldots, u[(m+1)L]$:
Output samples $\mathbf{z}_m = [z[mL+1] \ldots z[(m+1)L]]^{\mathrm{T}}$:

$$\mathbf{z}_m = [\mathbf{0} \;\; \mathbf{I}_L] \mathscr{F}^{-1} \sum_{p=0}^{L_{\hat{F}}/P-1} \mathbf{U}_p^{BP_1}[m] \hat{\mathbf{F}}_p[m]$$

with

$$\mathbf{U}_p^{BP_1}[m] = \mathrm{diag}\left\{ \mathscr{F} \begin{bmatrix} u^{BP_1}[(m+1)L - pP - M + 1] \\ \vdots \\ u^{BP_1}[(m+1)L - pP] \end{bmatrix} \right\}$$

and $u^{BP_1}[mL+i] = B_1(q)u[mL+i]$, $i = 1, \ldots, L$.
Pre-filtering of loudspeaker and microphone signals:

$$u^{\mathrm{f}}[mL+i] = B_2(q)u^{BP_1}[mL+i],$$

$$y^{\mathrm{f}}[mL+i] = B_2(q)y[mL+i], \quad i = 1, \ldots, L,$$

$$\mathbf{U}_p^{\mathrm{f}}[m] = \mathrm{diag}\left\{ \mathscr{F} \begin{bmatrix} u^{\mathrm{f}}[(m+1)L - pP - M + 1] \\ \vdots \\ u^{\mathrm{f}}[(m+1)L - pP] \end{bmatrix} \right\} \quad \forall p = 0 : \frac{L_{\hat{F}}}{P} - 1.$$

Update formula:

$$\mathbf{y}_m^{\mathrm{f}} = [y^{\mathrm{f}}[mL+1] \ \ \ldots \ \ y^{\mathrm{f}}[(m+1)L]]^{\mathrm{T}},$$

$$\mathbf{E}^{\mathrm{f}}[m] = \mathscr{F}\begin{bmatrix}\mathbf{0}\\ \mathbf{I}_L\end{bmatrix}\left(\mathbf{y}_m^{\mathrm{f}} - [\mathbf{0}\ \ \mathbf{I}_L]\mathscr{F}^{-1}\sum_{p=0}^{L_{\hat{F}}/P-1}\mathbf{U}_p^{\mathrm{f}}[m]\hat{\mathbf{F}}_p[m]\right),$$

$$\hat{\mathbf{F}}_p[m+1] = \hat{\mathbf{F}}_p[m] + \mathbf{\Delta}[m]\mathscr{F}\mathbf{g}\mathscr{F}^{-1}\mathbf{U}_p^{\mathrm{f,H}}[m]\mathbf{E}^{\mathrm{f}}[m].$$

The bandwidths of the filters $B_1(q)$ and $B_2(q)$ determine the efficiency of the bandlimited feedback canceller: the larger the bandwidth, the larger the frequency range where acoustic feedback is cancelled, but the smaller the improvement which comes from the bandlimited adaptation (i.e., reduced desired signal distortion, smaller misadjustment). To specify the bandwidth of $B_1(q)$ and $B_2(q)$, identification of the critical frequency region (e.g., during fitting) for different hearing aids and different hearing aid users is required. However, the critical frequency region expands with increasing gain in the forward path $G(q)$ as well as, e.g., with the presence of a telephone handset or hand palm close to the ear. Hence, to guarantee stability, the bandwidths of $B_1(q)$ and $B_2(q)$ should not be chosen too small.

Note that the filter $B_1(q)$ introduces a group delay d_{c_1} in the feedback cancellation path. The total delay $d_c = d_{c_1} + d_{c_2}$ in the feedback cancellation path should not exceed the delay in the acoustic feedback path, otherwise the feedback signal can not be cancelled [28]. To guarantee a small group delay and to save computational complexity, low-order elliptic IIR filters $B_1(q)$ and $B_2(q)$ are used in [28]. In this paper, a second-order elliptic IIR filter $B_1(q) = B_2(q)$ with a cut-off frequency of 1000 Hz and a stopband attenuation of 30 dB is used.

4. Adaptive feedback cancellers based on a model of the desired signal (PEMAFC)

The adaptive feedback cancellation techniques described in Section 3 exploit prior knowledge of the feedback path to improve the estimation accuracy of the standard CAF. In these techniques, signal distortion reduction is traded off against the ability to model variations in the feedback path. In [18,34–36], the bias of the standard CAF is reduced by incorporating a (stationary or time-varying) model of the desired signal $x[n]$ in the identification. The desired signal model is then used to pre-whiten the desired signal component in the microphone and the loudspeaker signals. This approach has been adopted from direct closed-loop system identification with the PEM [37,38].

4.1. Closed-loop identification of the feedback path with the direct method

For the time being, we assume that the desired signal $x[n]$ can be modelled as

$$x[n] = H(q,n)w[n], \tag{47}$$

with $w[n]$ a zero mean, white noise sequence and $H(q,n)$ monic and inversely stable. In the direct method of closed-loop identification, the open-loop system $\{F(q,n), H(q,n)\}$,

$$\begin{aligned} y[n] &= F(q,n)u_{\mathrm{l}}[n] + H(q,n)w[n],\\ &= \tilde{F}(q,n)u[n] + H(q,n)w[n], \end{aligned} \tag{48}$$

is identified from the loudspeaker signal $u_l[n]$ and the microphone signal $y[n]$ by an open-loop identification method, thereby ignoring the presence of the closed signal loop $G(q)$. Only some specific open-loop identification methods can be applied to closed-loop systems, such as the PEM [37,38]. The PEM produces an estimate $\hat{F}(q,n)$ and $\hat{H}(q,n)$ of the feedback path $\tilde{F}(q,n)$ and the desired signal model $H(q,n)$, respectively, by minimizing the energy of the so-called prediction error $e^f[n] = \hat{H}(q,n)^{-1}(y[n] - \hat{F}(q,n)u[n])$, i.e.,

$$\begin{aligned} J(\hat{\mathbf{f}}[n]) &= \varepsilon\{|\hat{H}(q,n)^{-1}(y[n] - \hat{F}(q,n)u[n])|^2\} \\ &= \varepsilon\{|y^f[n] - \hat{\mathbf{f}}^T[n]\mathbf{u}^f[n]|^2\}, \end{aligned} \tag{49}$$

where

$$\mathbf{u}^f[n] = [u^f[n] \;\; u^f[k-1] \;\; \ldots \;\; u^f[k - L_{\hat{F}} + 1]]^T, \tag{50}$$

$$y^f[n] = \hat{H}(q,n)^{-1}y[n], \quad u^f[n] = \hat{H}(q,n)^{-1}u[n]. \tag{51}$$

Minimization of Eq. (49) results in

$$\hat{\mathbf{f}}[n] = \varepsilon\{\mathbf{u}^f[n]\mathbf{u}^{f,T}[n]\}^{-1}\varepsilon\{\mathbf{u}^f[n]y^f[n]\}, \tag{52}$$

where $y^f[n]$ can be decomposed as (cf. Eq. (48)):

$$y^f[n] = \hat{H}(q,n)^{-1}x[n] + \tilde{F}(q,n)u^f[n]. \tag{53}$$

If $\hat{H}(q,n)$ equals the true desired signal model $H(q,n)$,

$$y^f[n] = w[n] + \tilde{F}(q,n)u^f[n]. \tag{54}$$

Since $w[n]$ is white and $G(q)$ contains a delay $d_G \geqslant 1$, $u^f[n]$ and $w[n]$ are then uncorrelated and hence, in the sufficient-order case, $\hat{\mathbf{f}}[n]$ results in an unbiased feedback path estimate.

From Eq. (52), it follows that $J(\hat{\mathbf{f}}[n])$ can be solved by performing standard adaptive filtering techniques on the pre-whitened data $y^f[n]$ and $u^f[n]$. This is illustrated in Fig. 5, where $A(q,n) = \hat{H}(q,n)^{-1}$. The update equation of the PBFD implementation corresponds to Eqs. (39)–(46) with now $y^f[n]$ and $\mathbf{u}^f[n]$ defined in Eqs. (50)–(51).

4.2. Desired signal model

4.2.1. Fixed desired signal model (PEMAFC-f)

In [18,34], the desired signal model $H(q,n)$ is approximated by a *fixed* low-pass all-pole filter $\hat{H}(q,n) = A^{-1}(q)$, which represents the long-term average spectrum of speech. A simple model for the average speech spectrum is a first-order all-pole model [30]:

$$\hat{H}(q,n) = \frac{1}{1 - \alpha q^{-1}}, \tag{55}$$

with $\alpha < 1$ (e.g., $\alpha = 0.9$). Algorithm 4 summarizes the PEMAFC-f.

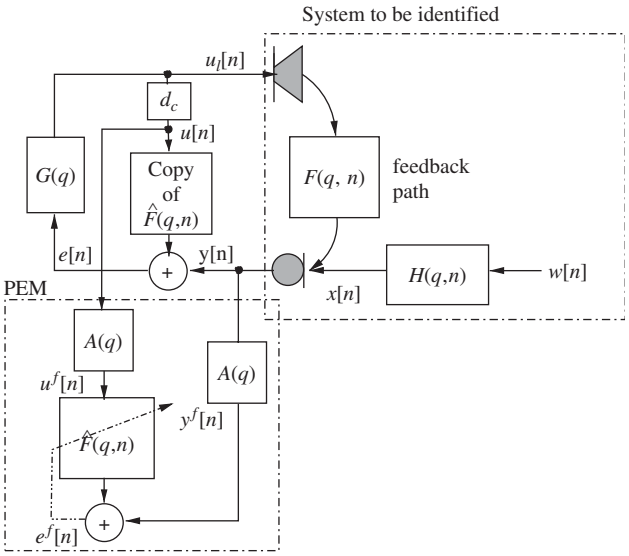

Fig. 5. Feedback cancellation with the prediction-error method.

Algorithm 4. PBFD implementation of PEMAFC-f.

For each block of L input samples $u[mL+1],\ldots,u[(m+1)L]$:
Output samples $\mathbf{z}_m = [z[mL+1]\ldots z[(m+1)L]]^{\mathrm{T}}$:

$$\mathbf{z}_m = [\mathbf{0}\ \ \mathbf{I}_L]\mathscr{F}^{-1}\sum_{p=0}^{L_{\hat{F}}/P-1}\mathbf{U}_p[m]\hat{\mathbf{F}}_p[m]$$

with

$$\mathbf{U}_p[m] = \mathrm{diag}\left\{\mathscr{F}\begin{bmatrix} u[(m+1)L-pP-M+1] \\ \vdots \\ u[(m+1)L-pP] \end{bmatrix}\right\}.$$

Pre-filtering of loudspeaker and microphone signals with $A(q) = 1-\alpha q^{-1}$:

$$u^{\mathrm{f}}[mL+i] = A(q)u[mL+i],$$

$$y^{\mathrm{f}}[mL+i] = A(q)y[mL+i], \quad i = 1,\ldots,L,$$

$$\mathbf{U}_p^{\mathrm{f}}[m] = \mathrm{diag}\left\{\mathscr{F}\begin{bmatrix} u^{\mathrm{f}}[(m+1)L-pP-M+1] \\ \vdots \\ u^{\mathrm{f}}[(m+1)L-pP] \end{bmatrix}\right\} \quad \forall p = 0 : \frac{L_{\hat{F}}}{P}-1.$$

Update formula:

$$\mathbf{y}_m^{\mathrm{f}} = [y^{\mathrm{f}}[mL+1] \ \ \ldots \ \ y^{\mathrm{f}}[(m+1)L]]^{\mathrm{T}},$$

$$\mathbf{E}^{\mathrm{f}}[m] = \mathscr{F}\begin{bmatrix}\mathbf{0}\\ \mathbf{I}_L\end{bmatrix}\left(\mathbf{y}_m^{\mathrm{f}} - [\mathbf{0}\ \ \mathbf{I}_L]\mathscr{F}^{-1}\sum_{p=0}^{L_{\hat{F}}/P-1}\mathbf{U}_p^{\mathrm{f}}[m]\hat{\mathbf{F}}_p[m]\right),$$

$$\hat{\mathbf{F}}_p[m+1] = \hat{\mathbf{F}}_p[m] + \mathbf{\Delta}[m]\mathscr{F}\mathbf{g}\mathscr{F}^{-1}\mathbf{U}_p^{\mathrm{f,H}}[m]\mathbf{E}^{\mathrm{f}}[m].$$

4.2.2. Adaptive desired signal model (PEMAFC-a)

In practice, the desired signal model $H(q,n)$ is unknown and highly time-varying. In addition, the quality of the feedback canceller $\hat{F}(q,n)$ strongly depends on the accuracy of the signal model estimate $\hat{H}(q,n)$ [34], so that it is desirable to identify the feedback path $F(q,n)$ as well as the desired signal model $H(q,n)$ with the PEM method. However, $F(q,n)$ and $H(q,n)$ are not always identifiable in the closed-loop system at hand [34]. In [36], we demonstrated that the desired signal model $H(q,n)$ and the feedback path $F(q,n)$ can be both identified in closed-loop (i.e. without adding non-linearities or a probe signal), if the total delay $d = d_G + d_c \geqslant L_{H^{-1}}$ with d_c the common delay in the feedback path $F(q)$ and the feedback cancellation path $q^{-d_c}\hat{F}(q)$.

Since many audio signals $x[n]$ can be approximated by a low-order AR model (cf. Section 2.1), we assume that

$$H^{-1}(q,n) = A(q,n) = 1 + q^{-1}\bar{A}(q,n) \tag{56}$$

with $\bar{A}(q)$ an FIR filter. For example, a 10–20 ms speech segment at a sampling frequency $f_s = 16\,\mathrm{kHz}$ can be modelled by a 10–20th order AR model with $w[n]$ a white noise excitation (in case of unvoiced sounds) or a pulse train excitation (in case of voiced sounds) [39]. The AR model $A(q,n)$ is computed through linear prediction of the feedback-compensated signal,

$$e[n] = y[n] - \hat{\mathbf{f}}^{\mathrm{T}}[n]\mathbf{u}[n]. \tag{57}$$

Note that $e[n] = x[n]$, if $\hat{\mathbf{f}}[n] = \tilde{\mathbf{f}}[n]$. In this paper, the AR model is estimated on subsequent frames of $N = 160$ samples (i.e., 10 ms) through the Levinson–Durbin algorithm [39]. The feedback canceller $\hat{F}(q,n)$ is then updated with the PBFD LMS algorithm using the updated AR model $\hat{H}^{-1}(q,n) = A(q,n)$ in Eqs. (50)–(51).

So far, we have assumed that the excitation of the desired signal model $H(q,n)$ is a white noise sequence $w[n]$. This assumption does not apply for voiced speech, where the excitation $w[n]$ approximates a pulse train that is periodical with the pitch period P (expressed as number of samples). Due to this periodicity, the pre-filtered loudspeaker signal $u^{\mathrm{f}}[n]$ is still correlated with the excitation signal $w[n]$ at the pitch frequency and its harmonics. From Eqs. (52)–(54), it follows that the feedback canceller $\hat{\mathbf{f}}[n]$ will then still be biased if

$$\varepsilon\{\mathbf{u}^{\mathrm{f}}[n]w[n]\} \neq 0. \tag{58}$$

Using $u^{f}[n] = \hat{H}^{-1}(q)q^{-d_c}C(q)x[n]$ with $\hat{H}^{-1}(q,n) = H^{-1}(q,n)$, it can be shown that (58) corresponds to

$$\varepsilon\{w[n-\delta]w[n]\} \neq 0 \tag{59}$$

for $d_G + d_c \leqslant \delta \leqslant L_C + L_{\hat{F}} + d_c - 2$. Hence, if

$$d_G + d_c \leqslant iP \leqslant L_C + L_{\hat{F}} - 2 \tag{60}$$

with $i \in \mathbb{N}_0$, the feedback path estimate will be biased at the frequencies if_s/P with $i/P < \frac{1}{2}$, where f_s equals the sampling frequency. For speech, the pitch frequency f_s/P lies between 50 and 400 Hz and hence, for $f_s = 16$ kHz, P lies between 40 and 320 samples. To remove the residual correlation caused by the pulse train excitation, a short-term AR model $A_{ST}(q,n)$ can be cascaded with a long-term predictor $A_{LT}(q,n) = (1 - bq^{-\hat{P}[n]})$, where $\hat{P}[n] \leqslant 320$ is an estimate of the pitch period P [40]:

$$A(q,n) = A_{ST}(q,n)(1 - bq^{-\hat{P}[n]}). \tag{61}$$

To guarantee identifiability, the delay $d_G + d_c \geqslant L_A = \hat{P}[n] + L_{A_{ST}}$ and, hence, $\hat{P}[n]$ should be constrained as

$$\hat{P}[n] \leqslant \min(d_G + d_c - L_{A_{ST}}, 320). \tag{62}$$

From Eqs. (60) and (62), it follows that the long-term predictor is especially useful for large delays $d_G + d_c$ (i.e., larger than 10 ms) and for long acoustic feedback paths (i.e., $L_{\hat{F}} \gg P$, e.g., in public-address applications) [40]. In hearing aids, the dominant part of the feedback path $F(q,n)$ is quite short, so that a relatively short filter length $L_{\hat{F}}$ (i.e., 50–100 taps) is typically used [9]. In addition, the delay d_G should be kept small. As a result, the benefit of a long-term predictor is limited for hearing aid applications. In the sequel, only a short-term AR model will therefore be used.

The equations of the PBFD implementation[3] of PEMAFC-a are summarized in Algorithm 5.

Algorithm 5. PBFD implementation of PEMAFC-a.

For each block of L input samples $u[mL+1], \ldots, u[(m+1)L]$:
Output samples $\mathbf{z}_m = [z[mL+1] \ldots z[(m+1)L]]^{T}$:

$$\mathbf{z}_m = [\mathbf{0}\ \ \mathbf{I}_L]\mathscr{F}^{-1} \sum_{p=0}^{L_{\hat{F}}/P-1} \mathbf{U}_p[m]\hat{\mathbf{F}}_p[m]$$

with

$$\mathbf{U}_p[m] = \operatorname{diag}\left\{ \mathscr{F} \begin{bmatrix} u[(m+1)L - pP - M + 1] \\ \vdots \\ u[(m+1)L - pP] \end{bmatrix} \right\}.$$

[3] In Algorithm 5, the loudspeaker and microphone signals are delayed by the framelength N before being used to update the feedback canceller [40] since $A(q,n)$ can only be computed at time $n = \tilde{m}N$.

Pre-filtering of loudspeaker and microphone signals with $A(q,\tilde{m}-1)$, $\tilde{m}=\lceil (mL+i)/N\rceil$:

$$u^{\mathrm{f}}[mL+i]=A(q,\tilde{m}-1)u[mL+i-N],$$

$$y^{\mathrm{f}}[mL+i]=A(q,\tilde{m}-1)y[mL+i-N],\quad i=1,\ldots,L,$$

$$\mathbf{U}_p^{\mathrm{f}}[m]=\mathrm{diag}\left\{\mathscr{F}\begin{bmatrix}u^{\mathrm{f}}[(k+1)L-pP-M+1]\\ \vdots\\ u^{\mathrm{f}}[(k+1)L-pP]\end{bmatrix}\right\}\quad \forall p=0:\frac{L_{\hat{F}}}{P}-1.$$

Update AR model $A(q,\tilde{m})$:
If $mL+i=\tilde{m}N$ with $\tilde{m}$ an integer and N the framelength:

$$A(q,\tilde{m})=\text{Levinson Durbin}([e[mL+i-N+1]\ \ \ldots\ \ e[mL+i]]^{\mathrm{T}})$$

with $e[mL+i]=y[mL+i]-z[mL+i]$.
Update formula:

$$\mathbf{y}_m^{\mathrm{f}}=[y^{\mathrm{f}}[mL+1]\ \ \ldots\ \ y^{\mathrm{f}}[(m+1)L]]^{\mathrm{T}},$$

$$\mathbf{E}^{\mathrm{f}}[m]=\mathscr{F}\begin{bmatrix}\mathbf{0}\\ \mathbf{I}_L\end{bmatrix}\left(\mathbf{y}_m^{\mathrm{f}}-[\mathbf{0}\ \ \mathbf{I}_L]\mathscr{F}^{-1}\sum_{p=0}^{L_{\hat{F}}/P-1}\mathbf{U}_p^{\mathrm{f}}[m]\hat{\mathbf{F}}_p[m]\right),$$

$$\hat{\mathbf{F}}_p[m+1]=\hat{\mathbf{F}}_p[m]+\mathbf{\Delta}[m]\mathscr{F}\mathbf{g}\mathscr{F}^{-1}\mathbf{U}_p^{\mathrm{f,H}}[m]\mathbf{E}^{\mathrm{f}}[m].$$

4.3. Improvement of the tracking performance with the shadow filter approach (PEMAFC-as)

The feedback canceller requires a slow convergence speed, and, hence, small step sizes $\bar{\mu}_k$, $k=0,\ldots M-1$, in order to obtain an accurate feedback path estimate at angular frequencies ω with a small loop gain $|G(\mathrm{e}^{\mathrm{j}\omega})F(\mathrm{e}^{\mathrm{j}\omega})|$. At those frequencies, the feedback signal to desired signal power ratio is small, resulting in a large misadjustment of the feedback canceller. On the other hand, a fast adaptation is required to track changes in the feedback path. To improve the tracking performance of the PEMAFC-a, a second faster adaptive filter $\hat{\mathbf{F}}_p^{\mathrm{Sh}}[m]$, $p=0,\ldots,L_{\hat{F}}/P-1$ (the so-called shadow filter) is put in parallel to the adaptive feedback canceller $\hat{\mathbf{F}}_p[m]$ [19]:

$$\hat{\mathbf{F}}_p^{\mathrm{Sh}}[m+1]=\hat{\mathbf{F}}_p^{\mathrm{Sh}}[m]+\mathbf{\Delta}^{\mathrm{Sh}}[m]\mathscr{F}\mathbf{g}\mathscr{F}^{-1}\mathbf{U}_p^{\mathrm{f,H}}[m]\mathbf{E}^{\mathrm{Sh,f}}[m],\tag{63}$$

$$\mathbf{E}^{\mathrm{Sh,f}}[m]=\mathscr{F}\begin{bmatrix}\mathbf{0}\\ \mathbf{I}_L\end{bmatrix}\left(\mathbf{y}_m^{\mathrm{f}}-[\mathbf{0}\ \ \mathbf{I}_L]\mathscr{F}^{-1}\sum_{p=0}^{L_{\hat{F}}/P-1}\mathbf{U}_p^{\mathrm{f}}[m]\hat{\mathbf{F}}_p^{\mathrm{Sh}}[m]\right),\tag{64}$$

$$\mathbf{\Delta}^{\mathrm{Sh}}[m]=\mathrm{diag}\left\{\frac{\bar{\mu}_0^{\mathrm{Sh}}}{P_{u^{\mathrm{f}},0}[m]+P_{\mathrm{e}^{\mathrm{f}},0}^{\mathrm{Sh}}[m]},\ldots,\frac{\bar{\mu}_{M-1}^{\mathrm{Sh}}}{P_{u^{\mathrm{f}},M-1}[m]+P_{\mathrm{e}^{\mathrm{f}},M-1}^{\mathrm{Sh}}[m]}\right\},\tag{65}$$

where $\bar{\mu}_k^{\mathrm{Sh}} > \bar{\mu}_k$, $k = 0, \ldots, M-1$, and

$$P_{e^f,k}^{\mathrm{Sh}}[m] = \frac{L_{\hat{F}}}{P} |E_{p,k}^{\mathrm{Sh,f}}[m]|^2. \tag{66}$$

When a change in feedback path occurs, the shadow filter $\hat{\mathbf{F}}_p^{\mathrm{Sh}}[m]$ converges faster than the feedback canceller $\hat{\mathbf{F}}_p[m]$ and hence, produces a better feedback path estimate. After convergence, the slower adapting feedback canceller $\hat{\mathbf{F}}_p[m]$ yields a smaller misadjustment and, hence, better steady-state performance than the shadow filter. To combine the advantages of the fast and slowly adapting filter, the average error power $\tilde{P}_{e^f,k}^{\mathrm{Sh}}$ and $\tilde{P}_{e^f,k}$ of the shadow filter and the feedback canceller in each frequency bin k are compared:

$$\tilde{P}_{e^f,k}[m] = \lambda \tilde{P}_{e^f,k}[m-1] + (1-\lambda) P_{e^f,k}[m], \tag{67}$$

$$\tilde{P}_{e^f,k}^{\mathrm{Sh}}[m] = \lambda \tilde{P}_{e^f,k}^{\mathrm{Sh}}[m-1] + (1-\lambda) P_{e^f,k}^{\mathrm{Sh}}[m], \tag{68}$$

where $\lambda < 1$ is an exponential weighting factor. If the shadow filter results in a smaller average error in a frequency bin, the filter coefficients of the shadow filter in this bin are copied to the feedback canceller. If, on the other hand, the shadow filter results in a larger average error in a frequency bin, the shadow filter coefficients in this bin are replaced by the coefficients of the slower adapting filter:

$$\hat{F}_{p,k}[m+1] = \hat{F}_{p,k}^{\mathrm{Sh}}[m+1] \quad \text{if } \tilde{P}_{e^f,k}^{\mathrm{Sh}}[m] < \alpha_k \tilde{P}_{e^f,k}[m], \tag{69}$$

$$\hat{F}_{p,k}^{\mathrm{Sh}}[m+1] = \hat{F}_{p,k}[m+1] \quad \text{if } \tilde{P}_{e^f,k}[m] < \beta_k \tilde{P}_{e^f,k}^{\mathrm{Sh}}[m], \tag{70}$$

where $\alpha_k \leqslant 1$ and $\beta_k \leqslant 1$ (e.g., $\alpha_k = 0.85$, $\beta_k = 0.87$).[4] In the sequel, the PEMAFC-a algorithm with shadow filter is referred to as PEMAFC-as.

The shadow filter approach assumes that the faster adapting filter only results in a smaller error when a change in the feedback path occurs [41]. Note that this assumption does not hold for the standard CAF algorithm, where the shadow filter will cancel desired signals with a temporarily strong autocorrelation. In the PEMAFC-a, cancellation of the desired signal is impeded through pre-whitening with an estimate of the instantaneous desired signal model $H(q,n)$. To improve the robustness of the shadow filter approach in scenarios where the adaptive estimate $A(q,n)$ only achieves partial decorrelation of $u[n]$ and $x[n]$, the feedback canceller is only replaced by the shadow filter if the shadow filter produces a smaller average error in at least $C > 1$ of the $M/2+1$ frequency bins.

In this paper, the step sizes $\bar{\mu}_k$ of the feedback canceller in PEMAFC-as are set three times smaller than the step sizes of the other algorithms (cf. Eq. (30)); the step sizes $\bar{\mu}_k^{\mathrm{Sh}}$ of the fast adapting shadow filter are set 15 times larger than the step sizes of the slowly adapting feedback canceller, i.e., $\bar{\mu}_k^{\mathrm{Sh}} = 15\bar{\mu}_k$. The parameter C is set to $\lceil (1600/2f_s)M \rceil$, where $\lceil x \rceil$ denotes the smallest integer larger than or equal to x.

[4] To avoid a continuous and a possibly erroneous switching between the slow and fast adapting filter, α_k and β_k should not be set too close to one. The slower adapting filter has a lower variance and is less sensitive to a possible residual correlation between $u^f[n]$ and $x^f[n]$. Therefore, the example value for β_k is larger than the value for α_k.

5. Simulation results

In this section, the different algorithms described in Sections 2, 3 and 4 are compared for acoustic feedback paths measured in two commercial BTE hearing aids, i.e., the GN Resound Canta 7 BTE (referred to as BTE 1) and the Siemens Acuris BTE Triano (referred to as BTE 2). Feedback paths of these two hearing aids have been measured in an office room. The hearing aids were attached to the right ear of a Cortex MK II artificial head. An earmold with a vent size of 2 mm was used. The feedback paths have been measured for two conditions, i.e., without obstruction and with a mobile phone attached to the head. The feedback paths from the loudspeaker to the first microphone of the BTEs are used in the simulations. The frequency responses of the feedback paths are depicted in Fig. 6 (a) and (b) for BTE 1 and 2, respectively. Since a different microphone amplification was used in the measurement setup of BTE 1 and 2, only the relative levels in the feedback path frequency responses are meaningful. The reference filter used in the C-CAF algorithm is also depicted. The reference filter was determined for the condition without obstruction. The feedback paths have a delay of 1 ms. The sampling frequency f_s equals 16 kHz.

The simulated feedback path filter length was set to 100 samples. The filter length $L_{\hat{F}}$ of the feedback canceller was set to 64 samples. The block length L of the PBFD implementation was set to 32, resulting in an algorithmic delay of 4 ms. The FFT length M was set to 64. The delay d_G in the forward path equals 5 ms (this includes the processing delay of the algorithm); the delay d_c in the cancellation path equals 1 ms.

5.1. Performance measures

To assess the performance of feedback cancellation algorithms we use the misalignment $\zeta(F(q,n),\hat{F}(q,n))$ between the true and estimated feedback path $\hat{F}(q,n)$ and the maximum and added stable gain [9].

The *misalignment* $\zeta(F(q,n),\hat{F}(q,n))$ is computed in the frequency domain as

$$\zeta_k(F(q,n),\hat{F}(q,n)) = 10\log_{10}\left(\frac{\int_0^{\pi}|F(e^{j\omega}) - e^{-j\omega d_c}\hat{F}(e^{j\omega})|^2\,d\omega}{\int_0^{\pi}|F(e^{j\omega})|^2\,d\omega}\right). \tag{71}$$

In [9], the *maximum stable gain* MSG is defined as the maximum allowable gain assuming a flat frequency response $G(q)$ for the hearing aid:

$$\mathrm{MSG} = 20\log_{10}\left(\min_{\omega}\frac{1}{|F(e^{j\omega}) - e^{-j\omega d_c}\hat{F}(e^{j\omega})|}\right). \tag{72}$$

The MSG is determined by the frequency where the mismatch between the true feedback path $F(q,n)$ and the feedback path estimate $q^{-d_c}\hat{F}(q,n)$ is largest. The system will however only be unstable when the phase at that frequency equals a multiple of 2π [3]. The *added stable gain* ASG is defined as the additional gain that is possible by using the feedback canceller $q^{-d_c}\hat{F}(q,n)$, i.e.,

$$\mathrm{ASG} = \mathrm{MSG} - 20\log_{10}\left(\min_{\omega}\frac{1}{|F(e^{j\omega})|}\right). \tag{73}$$

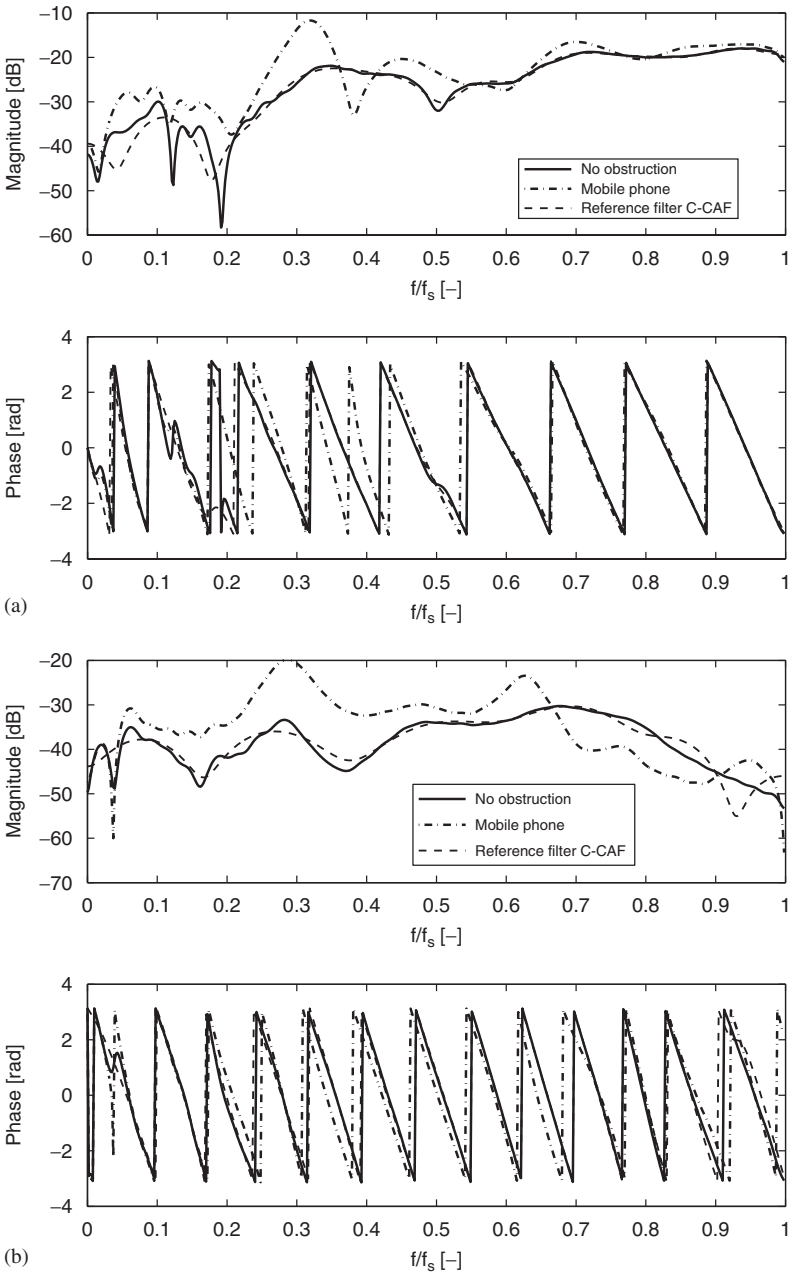

Fig. 6. Acoustic feedback paths of two commercial BTEs for two conditions, i.e., without obstruction and with a mobile phone attached to the head. The reference filter used in the C-CAF algorithm is also depicted. The sampling frequency $f_s = 16\,\text{kHz}$ (a) BTE 1; (b) BTE 2.

5.2. Simulation results

5.2.1. Stationary feedback path

Tables 1–4 depict the steady-state performance, i.e., the misalignment upon convergence, of the different algorithms for BTE 1 and 2, respectively. In Tables 1 and

Table 1
Misalignment of the different algorithms (CAF, C-CAF, BL-CAF, PEMAFC-f, PEMAFC-a, PEMAFC-as) for three different gains and BTE 1

	CAF	C-CAF	BL-CAF	PEMAFC-f	PEMAFC-a	PEMAFC-as
No obstruction:						
$G = 3$	2.6	−6.2	−3.0	−2.5	−3.7	−6.3
$G = 6$	−2.8	−9.7	−8.2	−8.1	−9.5	−11.6
$G = 14$	U	−14.7	−13.8	U	−16.6	−17.3
Mobile phone						
$G = 1$	7.8	−2.8	2.0	2.8	2.0	−1.5
$G = 3$	−0.0	−5.9	−5.7	−5.2	−6.4	−8.6
$G = 10$	U	U	U	U	−16.5	−16.2

U = unstable. Speech as a desired signal.

Table 2
Misalignment of the different algorithms (CAF, C-CAF, BL-CAF, PEMAFC-f, PEMAFC-a, PEMAFC-as) for three different gains and BTE 2

	CAF	C-CAF	BL-CAF	PEMAFC-f	PEMAFC-a	PEMAFC-as
No obstruction						
$G = 9$	3.1	−1.1	−0.1	−0.3	−0.9	−3.9
$G = 25$	−5.2	−8.0	−7.6	−9.0	−9.5	−10.5
$G = 40$	−8.6	−11.0	−10.2	−12.4	−13.2	−13.1
Mobile phone						
$G = 4$	3.4	−1.0	0.3	0.2	−0.4	−3.5
$G = 9$	−3.1	−4.9	−6.1	−6.7	−7.3	−9.5
$G = 20$	U	U	U	U	−13.5	−13.8

U = unstable. Speech as a desired signal.

Table 3
Misalignment of the different algorithms (CAF, C-CAF, BL-CAF, PEMAFC-f, PEMAFC-a, PEMAFC-as) for three different gains and BTE 1

	CAF	C-CAF	BL-CAF	PEMAFC-f	PEMAFC-a	PEMAFC-as
No obstruction						
$G = 3$	5.7	−4.4	3.0	1.3	0.3	−0.7
$G = 6$	0.1	−7.5	−2.3	−4.4	−5.6	−6.7
$G = 14$	U	−11.9	U	U	−12.7	−13.8
Mobile phone						
$G = 1$	11.5	−1.1	8.6	6.9	6.2	5.3
$G = 3$	3.0	−4.4	0.3	−1.4	−2.5	−3.5
$G = 10$	U	U	U	U	−12.7	−13.4

U = unstable. Music as a desired signal.

Table 4
Misalignment of the different algorithms (CAF, C-CAF, BL-CAF, PEMAFC-f, PEMAFC-a, PEMAFC-as) for three different gains and BTE 2

	CAF	C-CAF	BL-CAF	PEMAFC-f	PEMAFC-a	PEMAFC-as
No obstruction						
$G = 9$	9.4	3.4	7.7	5.4	4.1	2.8
$G = 25$	0.3	−3.4	−0.8	−3.2	−4.7	−5.2
$G = 40$	−3.9	−6.7	−4.6	−7.2	−8.7	−9.6
Mobile phone						
$G = 4$	9.9	2.1	7.7	5.9	4.7	4.2
$G = 9$	3.1	−1.2	1.3	−0.9	−2.2	−3.1
$G = 20$	U	U	U	U	−9.1	−9.8

U = unstable. Music as a desired signal.

2, the, the desired signal is a real speech signal consisting of HINT sentences produced by a male speaker [42]. The length of the speech signal equals 12 s. The speech signal was recorded in an office room at the first microphone of the two BTEs mounted on the artificial head. The loudspeaker was positioned at 1 m in front of the artificial head. In Tables 3 and 4, the desired signal is a music signal, consisting of a fragment (with a duration of 60 s) of 'Imagine' by John Lennon. The misalignment was averaged over the last 6 and the last 40 s of the simulations for the speech and the music signal, respectively. Three gains were considered in the experiments:

- A gain $|G(q)|$ below instability (i.e., for BTE 1, $|G| = 3$ and $|G| = 1$ for the condition without obstruction and with a mobile phone, respectively, and for BTE 2, $|G| = 9$ (without obstruction) and $|G| = 4$ (with a mobile phone), respectively).
- A gain $|G(q)|$ close to or at instability (i.e., for BTE 1, $|G| = 6$ and $|G| = 3$ for the condition without obstruction and with a mobile phone, respectively, and for BTE 2, $|G| = 25$ (without obstruction) and $|G| = 9$ (with a mobile phone), respectively).
- A gain $|G(q)|$ above the stability margin (i.e., for BTE 1, $|G| = 14$ and $|G| = 10$ for the condition without obstruction and with a mobile phone, respectively, and for BTE 2, $|G| = 40$ (without obstruction) and $|G| = 20$ (with a mobile phone), respectively).

For all test conditions, the standard CAF exhibits the largest misalignment ζ of all algorithms. The misalignment for the music signal is larger than for the speech signal because of a stronger correlation between $x[n]$ and $u[n]$. The performance of the algorithms generally improves with increasing gain $|G(q)|$ in the forward path. The larger the gain, the larger the feedback signal to desired signal power ratio, and, hence, the smaller the bias and misadjustment of the feedback cancellers caused by the desired signal (cf. Section 2.1).

For the speech signal and gains below or close to instability, the C-CAF, BL-CAF, PEMAFC-f and PEMAFC-a all have a similar steady-state performance: for the test scenario without obstruction, the C-CAF slightly outperforms the other approaches thanks to the prior knowledge of the feedback path. Unlike the C-CAF, BL-CAF and the PEMAFC-f, the PEMAFC-a algorithm however does not exploit assumptions about the feedback path or the desired signal model. For the music signal, the PEMAFC-a achieves a smaller misalignment than the BL-CAF and the PEMAFC-f.

For gains above the stability margin, the PEMAFC-a outperforms the BL-CAF, PEMAFC-f and the C-CAF, especially for the test scenario with a mobile phone. At high gains, a fast convergence is required in order to stabilize the system. Thanks to the pre-whitening operation, the PEMAFC-a exhibits a faster convergence speed (see Fig. 7), while the C-CAF, BL-CAF and PEMAFC-f are a lot slower and for some scenarios they are too slow to stabilize the unstable hearing aid (e.g., for the scenario with a mobile phone and a gain above the stability margin). The PEMAFC-as has the best performance among all algorithms. The PEMAFC-as combines a slower and a faster adaptive filter compared to the PEMAFC-a, resulting in a better steady-state performance than the PEMAFC-a, while guaranteeing a fast convergence speed for large gains.

Fig. 7 illustrates the convergence behaviour of all algorithms for $|G(q)| = 6$, BTE 1 without obstruction and the speech signal as a desired signal. The speech signal is depicted in Fig. 8. Fig. 7(a) depicts the convergence, i.e., misalignment as a function of time, of the CAF, the C-CAF and the BL-CAF. Of these three approaches, the BL-CAF exhibits the fastest convergence thanks to the filtering of the adaptation error with $B_2(q)$. Fig. 7(b) shows the convergence of the PEMAFC-f, PEMAFC-a and PEMAFC-as. The PEMAFC methods all pre-whiten the desired signal (which acts as a disturbance) to some extent, resulting in a faster convergence compared to the CAF, the C-CAF and the BL-CAF. Thanks to the adaptive estimate of the instantaneous speech model, the PEMAFC-a has a faster convergence than the PEMAFC-f. The PEMAFC-as initially switches to the fast adapting filter; afterwards, the slow adapting filter is used to further reduce the misalignment.

5.2.2. *Non-stationary feedback path*

To illustrate the tracking performance of the PEMAFC-as, an abrupt change of the feedback path was simulated after 3.75 s by switching the test conditions from a BTE mounted on the head without obstruction to a BTE on the head with a mobile phone attached to the head. Fig. 9 shows the tracking performance of the PEMAFC-a and the PEMAFC-as algorithm for BTE 1. Fig. 9(a) depicts the ASG of the PEMAFC-a as a function of time. Figure 9(b) depicts the ASG of the PEMAFC-as as a function of time. The ASG is depicted for three different forward path gains, i.e., $|G(q)| = 3$, $|G(q)| = 6$ and

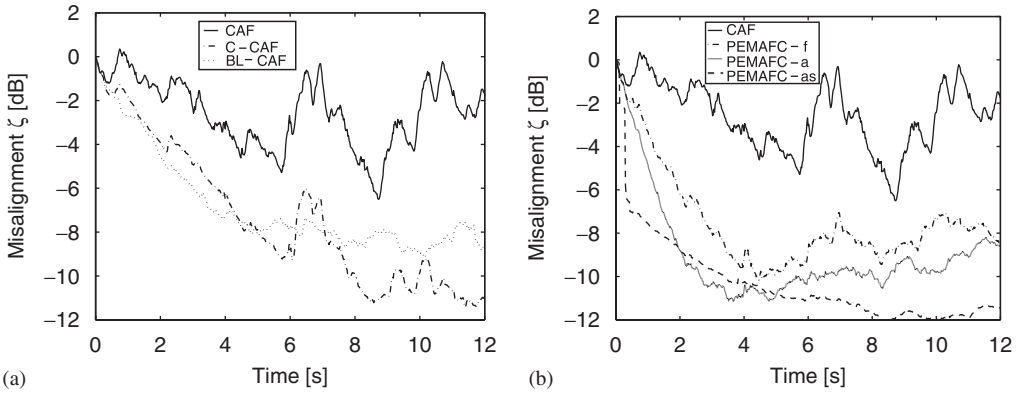

Fig. 7. Convergence (misalignment as a function of time) of the feedback cancellation algorithms. (a) CAF, C-CAF and BL-CAF and (b) CAF, PEMAFC-f, PEMAFC -a, PEMAFC-as.

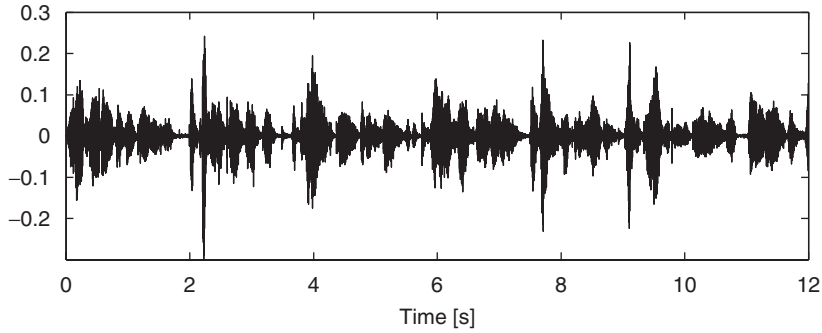

Fig. 8. Speech signal recorded at the first microphone of BTE 1.

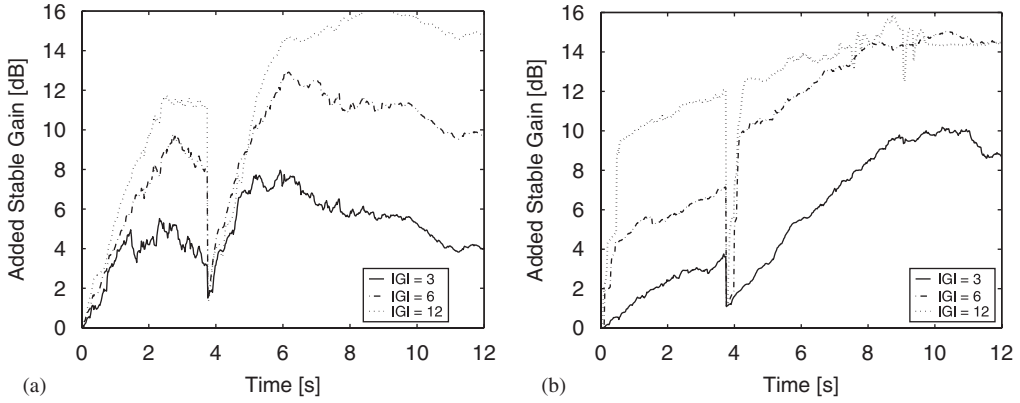

Fig. 9. Tracking performance (ASG as a function of time) of PEMAFC-a and PEMAFC-as for $|G(q)| = 3$, $|G(q)| = 6$ and $|G(q)| = 12$: (a) PEMAFC-a; and (b) PEMAFC-as.

$|G(q)| = 12$. For $|G(q)| = 6$ and $|G(q)| = 12$, the hearing aid system is unstable after the change (cf. Fig. 6(a)).

For high gains, the PEMAFC-as tracks abrupt changes in the feedback path faster than the PEMAFC-a. When a change in feedback path occurs, the PEMAFC-as automatically switches to the fast adapting shadow filter until a reasonable stability margin is reached. As a result, the PEMAFC-as restabilizes the unstable hearing aid system quicker than the PEMAFC-a. Subsequently, the PEMAFC-as switches back to the slower adapting filter to further improve the steady-state performance. The PEMAFC-as switches quicker to the fast adapting filter for high gains than for low gains. However, especially at high gains, a fast convergence is required because the system is close to or at instability. At low gains, the fast adapting filter has a bad accuracy because of the low feedback signal to desired signal power ratio, motivating the use of a slower adapting filter.

6. Conclusions

In general feedback cancellation setups, standard adaptive filtering techniques fail to provide a reliable feedback path estimate if the desired signal is spectrally colored because of the presence of a closed signal loop. In this paper, several approaches for improving the

estimation accuracy of the standard adaptive feedback canceller have been reviewed and compared, including constrained adaptation and bandlimited adaptation of the feedback canceller as well as adaptation with the PEM using a fixed or adaptive model of the desired signal. PBFD implementations of these algorithms have been compared for acoustic feedback paths measured in two commercial BTE hearing aids. The simulations showed that incorporating prior knowledge of the feedback path as well as exploiting an estimate of the desired signal in the adaptation improve the estimation accuracy of the standard feedback canceller. Thanks to a pre-whitening of the desired signal, the feedback cancellers based on a model of the desired signal exhibit a faster convergence than the feedback cancellers with constrained or bandlimited adaptation. In addition, we show that the shadow filter approach further improves the tracking performance of the PEMAFC with adaptive signal model. The PEMAFC with shadow filter combines a slow and a fast adaptive filter, resulting in a faster tracking of feedback path changes, while preserving a good steady-state performance.

Acknowledgments

Ann Spriet is a post-doctoral researcher supported by FWO-Vlaanderen. This research work was carried out at the laboratory of ESAT and ExpORL of the KU Leuven, in the frame of the European project HearCom ('Hearing in the communication society', WP5), the Belgian Programme on Interuniversity Attraction Poles, initiated by the Belgian Federal Science Policy Office IUAP P5/22 ('Dynamical systems and control: computation, identification and modelling'), the Concerted Research Action GOA-AMBIORICS ('Algorithms for medical and biological research, integration and software') of the Flemish Government and Research Project IWT project 040803 ('SMS4PA-II: sound management system for public-address systems'). The scientific responsibility is assumed by its authors.

References

[1] D.K. Bustamante, T.L. Worrall, M.J. Williamson, Measurement and adaptive suppression of acoustic feedback in hearing aids, in: Proceedings of the IEEE International Conference on Acoustics, Speech, and Signal Processing (ICASSP), vol. 3, Glasgow, Scotland, 1989, pp. 2017–2020.

[2] V. Hohmann, V. Hamacher, I. Holube, B. Kollmeier, T. Wittkop, Method for the operation of a hearing aid device or hearing device system as well as hearing aid device or hearing aid device system, US Patent, US 2002/0176595 A1, 2002.

[3] J.A. Maxwell, P.M. Zurek, Reducing acoustic feedback in hearing aids, IEEE Trans. Speech Audio Process. 3 (4) (1995) 304–313.

[4] R. Porayath, J. Daniel, Acoustic feedback elimination using adaptive notch filter algorithm, US Patent, US 5999631, 1999.

[5] R. Wang, R. Harjani, Acoustic feedback cancellation in hearing aids, in: Proceedings of the IEEE International Conference on Acoustics, Speech, and Signal Processing (ICASSP), vol. 1, Minneapolis, USA, 1993, pp. 137–140.

[6] J.L. Nielsen, U.P. Svensson, Performance of some linear time-varying systems in control of acoustic feedback, J. Acoust. Soc. Am. 1 (106) (1999) 240–254.

[7] M.R. Schroeder, Improvement of acoustic-feedback stability by frequency shifting, J. Acoust. Soc. Am. 36 (9) (1976) 1718–1724.

[8] J. Hellgren, T. Lunner, S. Arlinger, Variations in the feedback of hearing aids, J. Acoust. Soc. Am. 106 (5) (1999) 2821–2833.

[9] J.M. Kates, Room reverberation effects in hearing aid feedback cancellation, J. Acoust. Soc. Am. 109 (1) (2001) 367–378.
[10] B. Rafaely, M. Roccasalva-Firenze, E. Payne, Feedback path variability modeling for robust hearing aids, J. Acoust. Soc. Am. 107 (5) (2000) 2665–2673.
[11] M.R. Stinson, G.A. Daigle, Effect of handset proximity on hearing aid feedback, J. Acoust. Soc. Am. 115 (3) (2004) 1147–1156.
[12] J.E. Greenberg, P.M. Zurek, M. Brantley, Evaluation of feedback-reduction algorithms for hearing aids, J. Acoust. Soc. Am. 108 (5) (2000) 2366–2376.
[13] J.M. Kates, Feedback cancellation in hearing aids: results from a computer simulation, Signal Process. 39 (3) (1991) 553–562.
[14] Y. Park, D. Kim, I. Kim, An efficient feedback cancellation for multiband compression hearing aids, in: Proceedings of the 20th Annual International Conference on Engineering in Medicine and Biology Society, vol. 5, 1998, pp. 2706–2709.
[15] S. Thipphayathetthana, C. Chinrungrueng, Variable step-size of the least-mean-square algorithm for reducing acoustic feedback in hearing aids, in: IEEE Asia-Pacific Conference on Circuits and Systems, 2000, pp. 407–410.
[16] M.A. Stone, B.C.J. Moore, Tolerable hearing aid delays. I. Estimation of limits imposed by the auditory path alone using simulated hearing losses, Ear Hear. 20 (3) (1999) 182–191.
[17] S. Laugesen, K.V. Hansen, J. Hellgren, Acceptable delays in hearing aids and implications for feedback cancellation, J. Acoust. Soc. Am. 105 (2) (1999) 1211–1212.
[18] J. Hellgren, Analysis of feedback cancellation in hearing aids with filtered-X LMS and the direct method of closed loop identification, IEEE Trans. Speech Audio Process. 10 (2) (2002) 119–131.
[19] A. Mader, H. Puder, G. Schmidt, Step-size controls for acoustic echo cancellation filters—an overview, Signal Process. 80 (9) (2000) 1697–1719.
[20] L. Ljung, T. Söderström, Theory and Practice of Recursive Identification, MIT Press, Cambridge, MA, 1983.
[21] T. Fillon, J. Prado, Acoustic feedback cancellation for hearing-aids, using multi-delay filter, in: Fifth Nordic Signal Processing Symposium (NORSIG), on board Hurtigruten, Norway, 2002.
[22] A. Kaelin, A. Lindgren, S. Wyrsch, A digital frequency-domain implementation of a very high gain hearing aid with compensation for recruitment of loudness and acoustic echo cancellation, Signal Process. 64 (1) (1998) 71–85.
[23] J.-S. Soo, K. Pang, Multidelay block frequency domain adaptive filter, IEEE Trans. Acoust. Speech Signal Process. 38 (4) (1990) 788–798.
[24] J.E. Greenberg, Modified LMS algorithms for speech processing with an adaptive noise canceller, IEEE Trans. Speech Audio Process. 6 (4) (1998) 338–350.
[25] T. Kaulberg, A hearing aid with an adaptive filter for suppression of acoustic feedback, European Patent, EP 1191814, 2002.
[26] J. Nielsen, M. Ekelid, Feedback cancellation using bandwidth detection, WO Patent, WO 01/06746 A2, 2001.
[27] J. Nielsen, M. Ekelid, Feedback cancellation with low frequency input, WO Patent, WO 01/06812 A1, 2001.
[28] H.-F. Chi, S.X. Goa, S.D. Soli, A. Alwan, Band-limited feedback cancellation with a modified filtered-X LMS algorithm for hearing aids, Speech Commun. 39 (1–2) (2003) 147–161.
[29] J.M. Kates, Constrained adaptation for feedback cancellation in hearing aids, J. Acoust. Soc. Am. 106 (2) (1999) 1010–1019.
[30] J.M. Kates, Adaptive feedback cancellation in hearing aids, in: J. Benesty, Y. Huang (Eds.), Adaptive Signal Processing: Applications to Real-World Problems, Springer, Berlin, 2003, pp. 23–55 (Chapter 2).
[31] B. Rafaely, N.A. Shusina, J.L. Hayes, Robust compensation with adaptive feedback cancellation in hearing aids, Speech Commun. 39 (1–2) (2003) 163–170.
[32] J. Hellgren, T. Lunner, S. Arlinger, System identification of feedback in hearing aids, J. Acoust. Soc. Am. 105 (6) (1999) 3481–3496.
[33] A. Spriet, I. Proudler, M. Moonen, J. Wouters, An instrumental variable method for adaptive feedback cancellation in hearing aids, in: Proceedings of the IEEE International Conference on Acoustics, Speech, and Signal Processing (ICASSP), vol. 3, Philadelphia, PA, USA, 2005, pp. 129–132.
[34] J. Hellgren, U. Forssell, Bias of feedback cancellation algorithms in hearing aids based on direct closed loop identification, IEEE Trans. Speech Audio Process. 9 (7) (2001) 906–913.
[35] R. Leber, W. Schaub, Circuit and method for the adaptive suppression of an acoustic feedback, US Patent, US 6611600, 2003.

[36] A. Spriet, I. Proudler, M. Moonen, J. Wouters, Adaptive feedback cancellation in hearing aids with linear prediction of the desired signal, IEEE Trans. Signal Process. 53 (10 (Part 1)) (2005) 3749–3763.
[37] U. Forssell, Closed-loop identification—methods, theory and applications, Ph.D. Thesis, Linköping Universitet, Linköping, Sweden, 1999.
[38] U. Forssell, L. Ljung, Closed-loop identification revisited, Automatica 35 (1999) 1215–1241.
[39] J.R. Deller, J.G. Proakis, J.H.L. Hansen, Discrete-Time Processing of Speech Signals, Macmillan Publishing Company, Englewood Cliffs, NJ, 1993.
[40] G. Rombouts, T. van Waterschoot, K. Struyve, M. Moonen, Acoustic feedback suppression for long acoustic paths using a nonstationary source model, IEEE Trans. Signal Process 54 (9) (2006) 3426–3434.
[41] H. Puder, B. Beimel, Controlling the adaptation of feedback cancellation filters—problem analysis and solution approaches, in: Proceedings of the European Signal Processing Conference (EUSIPCO), Vienna, Austria, 2004, pp. 25–28.
[42] M. Nilsson, S.D. Soli, A. Sullivan, Development of the hearing in noise test for the measurement of speech reception thresholds in quiet and in noise, J. Acoust. Soc. Am. 95 (2) (1994) 1085–1099.